IEEE Robotics and Automation Letters (RAL) paper presented at
2024 IEEE/RSJ International Conference on Intelligent Robots and Systems (IROS)
October 14-18, 2024. Abu Dhabi, UAE

Rail DRAGON: Long-reach Bendable Modularized Rail Structure for Constant Observation inside PCV

Ryota Yokomura*[1], Masataka Goto*[1], Takehito Yoshida*[1],
Shin'ichi Warisawa*[1], Toshihide Hanari*[2], Kuniaki Kawabata*[2], and Rui Fukui*[1].

***Abstract*—To reduce errors in the remote control of robots during decommissioning, we developed a Rail DRAGON, which enables continuous observation of the work environment. The Rail DRAGON is constructed by assembling and pushing a long rail structure inside the primary containment vessel (PCV), and then repeatedly deploying several monitoring robots on the rails to enable constant observation in a high-radiation environment. In particular, we have developed the following components of Rail DRAGON: bendable rail modules, straight rail modules, a basement unit, and monitoring robots. Concretely, this research proposes and demonstrates a method to realize an ultralong articulated structure with high portability and workability. In addition, it proposes and verifies the feasibility of a method for deploying observation equipment that can be easily deployed and replaced, while considering disposal.**

***Index Terms*—Mechanism Design, Actuation and Joint Mechanisms, Robotics in Hazardous Fields, Distributed Robot Systems**

I. Introduction

THE Great East Japan Earthquake caused a severe accident at the Fukushima Daiichi Nuclear Power Station. To date, Tokyo Electric Power Company Holdings, Inc. has made various efforts to decommission its plants. Furthermore, it is important to remove radioactive fuel debris inside the PCV of Unit 2. The operation is difficult for humans to perform because of the high radiation environment, and robots are required. Various robots have been deployed for decommissioning, but some have become unrecoverable owing to remote control failures caused by a lack of information in the workspace [1]. To reduce teleoperation errors, it is effective to present the operator with images of the robot and its surrounding environment from multiple viewpoints [2].

Manuscript received: August, 6, 2023; Revised December, 24, 2023; Accepted February, 9, 2024.

This paper was recommended for publication by Editor M. Ani Hsieh upon evaluation of the Associate Editor and Reviewers' comments. This work was supported by the Nuclear Energy Science & Technology and Human Resource Development Project (through concentrating wisdom) from the Japan Atomic Energy Agency / Collaborative Laboratories for Advanced Decommissioning Science.

[1]Ryota Yokomura, Masataka Goto, Takehito Yoshida, Shin'ichi Warisawa, and Rui Fukui are with Department of Human and Engineered Environmental Studies, School of Frontier Science, the University of Tokyo, Chiba, 277-8563, Japan. yokomuraryota@lelab.t.u-tokyo.ac.jp; masa.shiraoka904@gmail.com; tyoshida@edu.k.u-tokyo.ac.jp; warisawa@edu.k.u-tokyo.ac.jp; fukui@ra-laboratory.com

[2]Toshihide Hanari and Kuniaki Kawabata are with Remote System and Sensing Technology Division, Collaborative Laboratories for Advanced Decommissioning Science (CLADS), Sector for Fukushima Research & Development, Japan Atomic Energy Agency (JAEA), Fukushima, 979-0513, Japan. hanari.toshihide@jaea.go.jp; kuniakik@icloud.com

Digital Object Identifier (DOI): see top of this page.

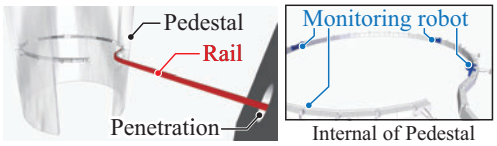

Fig. 1. Concept of Rail DRAGON.

Continuous observation inside the PCV is necessary for safe and long-term decommissioning to remove fuel debris.

It is necessary to pass through narrow areas to access the interior of the PCV. The deformable robot "PMORPH"[3] changes its shape when it passes through a hole and can run on the floor. Therefore, it can pass through narrow areas and run stably on the grating. A snake-shaped robot [4] was developed to investigate the interior of underground mines, which are similarly narrow environments. However, inside the PCV, the large steps and unstable road surfaces caused by melted grating inhibit access by running on the floor.

Endo et al. have developed "Super Dragon," a long manipulator [5]. Super Dragon uses a wire interference drive mechanism to install all motors at the base of the arm, reducing the overall weight of the arm and enabling the control of a 10-m-long articulated arm. An observation device can be attached to the end of the arm to observe the interior of the PCV. However, the entire arm must be retracted when the observation equipment malfunctions because of radiation.

Ueno et al. have developed a thruster-driven long manipulator, "Hiryu-2" [6]. Hiryu-2 uses thrusters to drive the joints and compensate for their weight to realize a long structure. However, thrusters can scatter radioactive materials into the air inside PCV. JET-FEDA developed an 8 m long horizontal articulated arm, "Octant", for the maintenance of the Joint European Torus [7]. The octant comprises five parts connected by five vertical-axis joints and can support a load of 100 kg at the tip. It weighs approximately 7,000 kg, making it difficult to transport into a building.

Fukui developed an automated rail-structure construction system [8] that allows the robot to construct a long structure by extending the rail on which it moves. The robot can support its weight by geometrically fixing its structure to the floors and walls using leg modules. This system is modular and portable, but several days are required to construct considerable modules using a teleoperated robot.

Therefore, this study proposes and verifies the feasibility of "Rail DRAGON" (Fig. 1), a bendable, ultra-long modular rail structure system that is easy to construct and portable for easy installation and disposal of observation equipment.

The contributions of this study are as follows. (1) Proposal of a method for realizing an ultralong articulated arm with high portability and ease of installation. To realize a long articulated arm, the power of the joint actuator was reduced by correcting the tilt of the joint axes. The modularized arm is not rigidly fixed but is supported by rollers and extruded to improve portability and workability. (2) It proposes a method for the easy installation and disposal of observation equipment on the arm. The monitoring robot was supported by a plate on the side of the rail in the overhang state without being completely restrained. A mechanism was provided to interpolate the side plates at the joints according to the joint angles. These devices enable the smooth movement of a concise monitoring robot. Furthermore, a mechanism with variable back drivability using magnetic coupling was developed to facilitate the recovery and disposal of a malfunctioned robot.

II. Continuous Observation by Rail DRAGON

In this section, we examine a method of deploying an ultra-long articulated structure that realizes constant observation and an observation device that can be easily deployed and replaced. We discuss the required functions in Section IIA, describe the ultra-long articulated structure in Section IIB, and describe the monitoring robot in Section IIC.

A. Monitoring in high radiation environments

To achieve continuous observation, the following functions are required: (1) Access to the interior of the pedestal. (2) Capability to address observation equipment failures owing to high-radiation environments. (3) Multi-perspective monitoring of robot operational environment.

In high radiation environments, observation equipment that utilizes semiconductors is expected to fail within a short period [9]. Therefore, it is crucial to have the ability to replace the observation equipment easily. For Rail DRAGON, a robot equipped with observation devices (as a monitoring robot) moves along the rail structure installed inside the PCV. This enables the convenient replacement of the observation equipment.

B. Installation of rail structure inside the pedestal

To introduce a long cantilevered-rail structure, the following functions must be achieved: (Rq-r.1) Support for large moments and loads: (Rq-r.2) Portability of equipment and shortened construction time. (Rq-r.3) Avoid various obstacles.

1) Supporting large moments and loads: We assume that a 0.5 m diameter through-hole is provided to access the inside of the PCV. The distance from the through hole to the pedestal was 7 m. In addition, the grating that serves as a scaffold inside the PCV has partially fallen off. Therefore, the rail structure cannot be anchored to the grating to support its weight in the middle of the structure. Therefore, the rail is cantilevered.

2) Portability and reduction of assembling time: Securing a route for carrying large and heavy machines assembled outside a building is challenging, and the speed of movement is slow. Therefore, the structure is divided into modules of size and weight that can be carried manually to increase portability [10]. To reduce the risk of work failure and shorten the installation time, workers connect the modules to the base of the rail structure and push them out using a machine (Fig. 2).

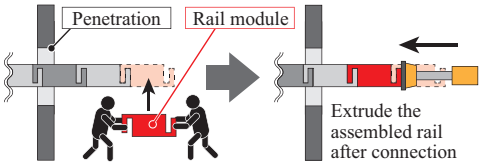

Fig. 2. Connection and extrusion of rail module.

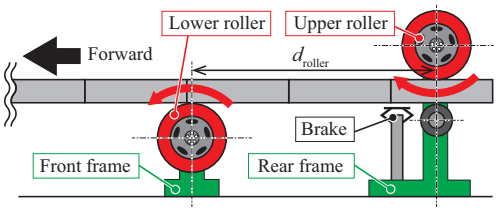

Fig. 3. Basement unit using two large rollers.

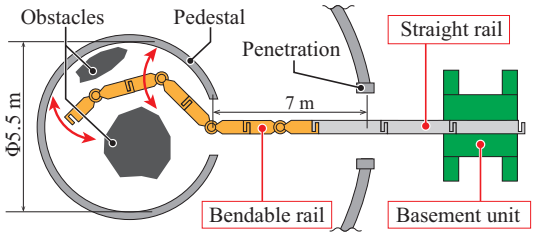

Fig. 4. Obstacle avoidance using active joints.

Large moments and loads are supported in the basement unit. In addition, the rail structure could not be fixed because of the sequential extrusion process. Therefore, the rail is supported by two rollers at a sufficiently long distance d_{roller}, as shown in Fig. 3. Additionally, the frame was divided for each roller to ensure portability.

3) Obstacle avoidance: Previous investigations in the PCV revealed that part of the floor (grating) has collapsed, and the radioactive debris has fallen to the bottom, but no major obstacles remain on the grating in the PCV[11]. However, there may be unknown damaged areas or obstacles inside the PCV, the tip of the rail structure was divided into bendable rails, and the root side into straight rails, as shown in Fig. 4. Each module of the bendable rail structure has a 1-DOF active joint that can move horizontally. The entire rail structure is operated as an articulated arm to avoid obstacles.

When the rail structure bends, a moment is generated around the center of the rail, and the rail structure twists as with other SCARA robots [12], increasing the angle θ_{twist} as shown in Fig. 5. This adds torque owing to gravity to the joint axis and increases the rotational torque required by the actuator. Specifically, as the torsional angle of the rail structure increased, it became more difficult to drive the joint. We attempted to solve this problem by improving the specific rigidity of the straight module and realizing a roll-angle adjustment function in the basement unit.

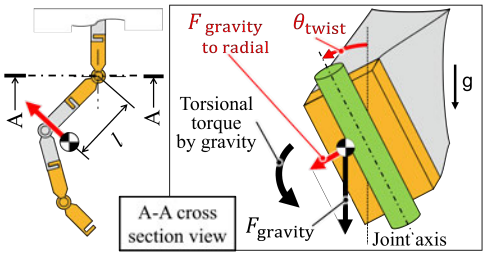

Fig. 5. Tilt of joint axis by torsion of rail.

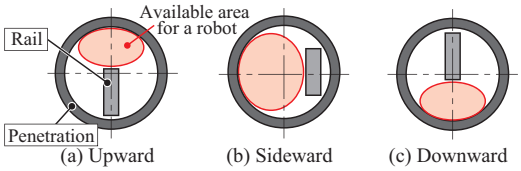

Fig. 6. Comparison of monitoring robot position.

C. Easy introduction and disposal of monitoring robots

Multiple monitoring robots are deployed on the rail structure and must constantly observe the PCV interior, even in the event of failure. This requires easy fabrication and handling of the failed monitoring robots.

1) Easy production and introduction of monitoring robots: Since a high-radiation environment renders monitoring robots unusable in a short period, it is necessary to realize low-cost monitoring robots that can be deployed repeatedly. The structure of the monitoring robot is simplified for low cost and disposability.

Next, the space through which the monitoring robot could pass was considered. Because the robot inserts into the PCV through a 0.5 m-diameter through-hole, there are three possible areas: upward, sideward, and downward, as shown in Fig. 6. Considering that the cross-section of the rail structure is longitudinal to increase the cross-sectional secondary moment of the rail structure and the size of the PCV penetration hole, the robot can use the space most effectively when it is on the side, as shown in Fig. 6 (b).

When the monitoring robot travels along the side of the structure, it should not consume power to support its weight, and it should be easy to place the robot on the rail for repeated introduction. Therefore, an overhanging structure is adopted. Compared to the case in which the monitoring robot is completely constrained in one axis direction, this structure allows for a larger positioning error of robot introduction.

If the robot is caught on a rail as shown in Fig. 7 (a), the monitoring robot will interfere with the pedestal wall when the rail comes in contact with the pedestal wall. Therefore, as illustrated in Fig. 7 (b), the robot is caught by a plate (red part in Fig. 7) attached to the side of the rail structure.

2) Easy disposal of monitoring robots: Monitoring robots contaminated with radioactive materials are disposed of as radioactive waste [13]. Because several monitoring robots are deployed for continuous observation, numerous wastes are generated. To facilitate disposal, a low degree of radioactive contamination or a low percentage of contaminated parts is

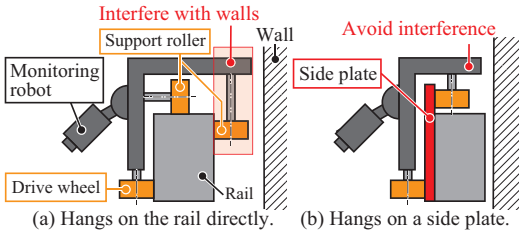

Fig. 7. Monitoring robot hangs on a side plate of rail.

desirable. Therefore, the monitoring robot is covered with a non-adhesive bag, such as a plastic bag.

The disposal procedure is as follows: Step 1. The monitoring robot covered by the bag is washed with high-pressure water; Step 2. The bag and monitoring robot are separated using a remote-controlled robot; Step 3. The bag is disposed of as radioactive waste, and the monitoring robot is disposed of as regular waste. By preventing radioactive materials from adhering to the main body of the monitoring robot with the bag, the number of contaminated parts can be reduced, and the disposal of costly radioactive waste can be reduced.

The following two tasks must be achieved when the monitoring robot is covered with a bag: Task (a) Smooth movement of the robot sealed with a bag. Task (b) Easy attachment and removal of bags using a remote-controlled robot for disposal.

For Task (a), the monitoring robot and rail structure are in contact with each other through the drive wheels and support rollers, and the robot moves by the frictional force of the drive wheels. Therefore, drive wheels and support rollers must be mounted outside the bag. When connecting the main body of the robot and drive wheels with a shaft, a hole is required in the part of the bag, and the sealing property of the bag is compromised. Therefore, magnetic coupling is used to transmit torque from the inside of the bag to drive the wheels placed outside the bag.

For Task (b), fastening with bolts did not satisfy Task (a), because it required a hole in the bag. In addition, if the bag is fixed using an adhesive, the resin may deteriorate owing to radiation and decompose unintentionally. Therefore, multiple support rollers are attached to a single sheet metal part, and the sheet metal part is fixed to the monitoring robot covered by the bag using clips.

3) Easy retrieval of monitoring robots: When a monitoring robot malfunctions, it is removed from the rail so as not to interfere with other robots and is retrieved for disposal. Because the rail is a single track, and it is difficult for robots to pass each other, it is impossible to deploy a dedicated robot to tow the failed robot. As illustrated in Fig. 8, a waste storage can is supported by another waste-handling robot near the end of the rail structure. A healthy monitoring robot propels the failed robot, and the failed robot is pushed out from the end of the rail and placed in the storage can. Finally, the waste-handling robot retrieves the can.

There are three methods for achieving the propulsion of a failed robot. (Prop. A) Install an actuator and an energy source that operate only when propulsion is required. (Prop. B) Use of a mechanism with high back drivability. (Prop. C)

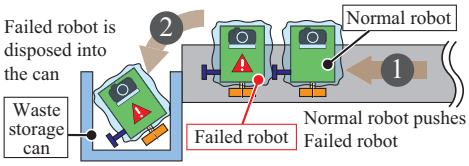

Fig. 8. Monitoring robot propelled by another robot.

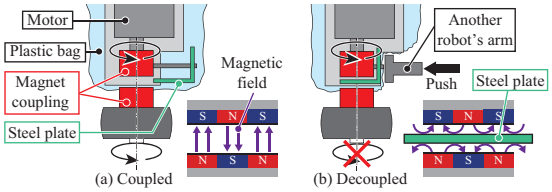

Fig. 9. Torque shut-off mechanism using magnet coupling and steel plate.

Use a mechanism with low back drivability when the vehicle is healthy but high back drivability only when it is propelled. In (Prop. A), the healthy robot pressed a switch to activate the actuator to move the failed robot. However, this is not feasible because it is necessary to maintain the integrity of the electrical components used for propulsion against radiation. Several mechanisms can be employed to achieve this (Prop. B), such as direct-drive actuators [14] and electrostatic actuators [15]. However, when the rail is tilted, it is difficult for a healthy monitoring robot to remain stationary without electric power. The standard means of realizing (Prop. C) is a clutch, which requires additional electrical components. However, magnetic coupling, such as that used in a power shut, can change the magnetic field by inserting an iron plate between the two components, thereby suppressing torque transmission(Fig. 9). This method does not interfere with the healthy operation of the coupling and can be realized only with the addition of mechanical parts, thereby minimizing the risk of failure owing to radiation. The exposure of permanent magnets to radiation leads to demagnetization[16]. However, this study does not consider the effect of radiation on permanent magnets, as the electronic components are more likely to fail due to radiation before any significant demagnetization occurs. Therefore, a method using magnetic coupling and iron plates was adopted.

III. Development of Straight Rail Structure and Basement Unit

The bendable rail structure is connected to the straight rail modules, and the straight rail modules are supported by the basement unit (Fig. 10). In our final design and goal, Rail DRAGON consists of five bendable modules and ten straight modules with a total length of 17.5 m. A monitoring robot is introduced from the basement unit that can move on the bendable and straight rail structures.

A. Development of bendable rail module

The required features of the bendable rail module are as follows. (Rq-b.1) Lightweight and rigid sufficient to withstand its weight and the load of the monitoring robot. (Rq-b.2) Easy to connect. (Rq-b.3) can be bendable.

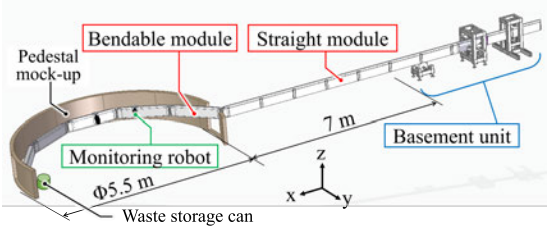

Fig. 10. Overview of developed "Rail DRAGON".

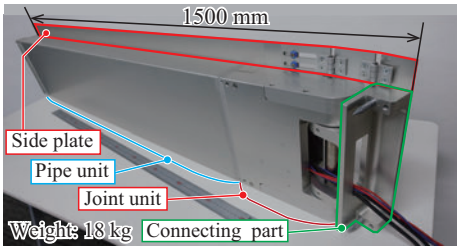

Fig. 11. Overview of developed bendable rail module.

To achieve (Rq-b.1), the bendable module must have high rigidity. The main components of the rail structure should be pipe structures with large cross-sectional secondary moments and small cross-sectional areas because the rail has a rectangular cross-sectional shape for the passage of the monitoring robot. To achieve (Rq-b.2), the connection between the modules and between joints and pipe structures should be the same such that the connection work can be standardized. A motor is installed on the module to achieve the (Rq-B.3).

1) Basic design of bendable rail module: A bendable rail module is shown in Fig. 11. The bendable rail module comprises a pipe structure and joint part. Each end has a connector. One side of the structure is equipped with a plate to monitor the robot.

2) Joint unit: The joint drive is illustrated in Fig. 12. The shaft is rotated using a timing belt from a Maxon geared motor (RE40+GP52C, 144 W) with a continuous torque of 30 Nm. A potentiometer (RV24YN20S made by Tokyo Cosmos Electric Co.) is installed on the opposite side of the shaft to measure the joint angle. The wiring of the motor and potentiometer is routed from the inside of the module to the connecting surface. The difference between the target joint angle and the present joint angle determines the target angle speed ω_{t} based on Eq. (1) where θ is the joint angle, θ_{t} is the target joint angle, e_{th} is the threshold. Velocity proportional-integral (PI) control was used to control each joint as shown in Eq. (2). To prevent a large moment of inertia caused by the long rail from increasing the speed undesired, only on the third joint, the p-gain (K_{P}) is smaller and the I-gain (K_{I}) is larger than the other joints because the inertia of the entire rail is large, and stable control is required.

$$\omega_{\mathrm{t}} = \begin{cases} \omega_{\max} & \text{if } \theta - \theta_{\mathrm{t}} > e_{\mathrm{th}} \\ \omega_{\max} \times \dfrac{\theta - \theta_{\mathrm{t}}}{e_{\mathrm{th}}} & \text{if } |\theta - \theta_{\mathrm{t}}| \leq e_{\mathrm{th}} \\ -\omega_{\max} & \text{if } \theta - \theta_{\mathrm{t}} < -e_{\mathrm{th}} \end{cases} \tag{1}$$

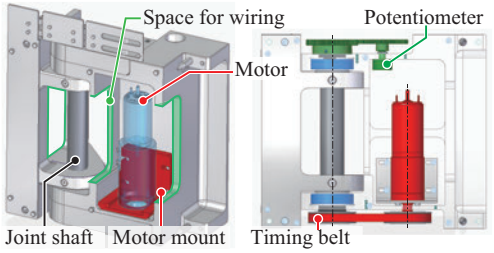

Fig. 12. Detail view of joint unit actuator.

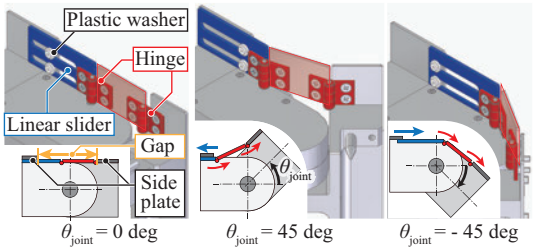

Fig. 13. Overview of side plate interpolation mechanism.

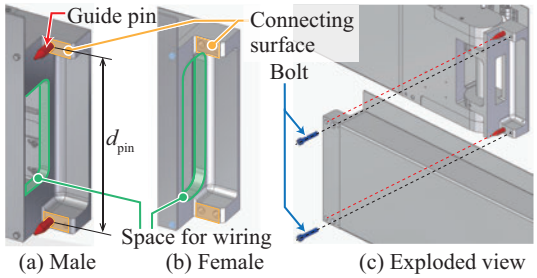

Fig. 14. Overview of connecting part.

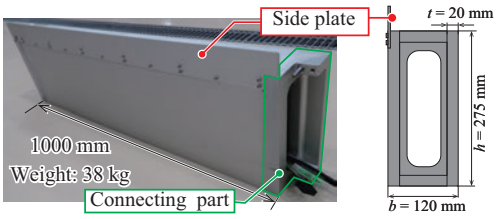

Fig. 15. Overview of designed straight module.

$$V = K_{\mathrm{P}}(\omega_{\mathrm{t}} - \omega) + K_{\mathrm{I}} \int (\omega_{\mathrm{t}} - \omega)\mathrm{d}t \tag{2}$$

3) Side plate: The monitoring robot moves overhanging a side plate attached to the side of the module as shown in Fig. 7. When the joint angle θ_{joint} changes, the relative positions of the side plates change significantly, as shown in Fig. 13, and when $\theta_{\mathrm{joint}} = -45$ deg, the support roller of the monitoring robot is de-wheeled owing to the large gap.

To address this problem, we developed a mechanism that fills the gap between the side plates (Fig. 13). This mechanism comprises two hinges and a linear slider with plastic washers. Along the joint axis, this mechanism operates as a slider-crank mechanism. Using a link mechanism, the mechanism can respond to continuous changes in the joint angle.

4) Connecting part: The connecting part of the module is shown in Fig. 14. The requirements of the connecting parts are (Rq-c.1) easy connection by workers, (Rq-c.2) strength to withstand loads from large moments, and (Rq-c.3) space for wiring the joint actuators.

In (Rq-C.1), the connection work can be divided into alignment and fastening. For alignment, two guide pins (ϕ 10, made of SKS2) are used. For fastening, a bolt fixation is used, which is removable and can fasten firmly. In this case, because the guide pins support the load applied to the connection, only the surface to which they are attached (the orange surface in Fig. 14) should be contacted to avoid excessive restraint. To support large loads, the bolts are placed such that they are not subjected to shear forces. The connection part has a staircase shape, with one surface in contact and two guide pins attached at a long distance $d_{\mathrm{pin}} = 255$ mm on the top and bottom to support the load. when the torque applied to the connection of the module at the root is $T = 18(\mathrm{kg}) \times 5 \times 3.75(\mathrm{m}) \times 9.8(\mathrm{m/s^2}) = 3.3$ kNm, the shear force on the pin is $F_{\mathrm{shear}} = T/d_{\mathrm{pin}} = 13$ kN, and smaller than guide pin's yield stress (120 kN). Two bolts are used to fasten the structure from the sides to improve workability.

The center of the structure is hollowed out (green hole in Fig. 14) to create a pipe structure, which reduces weight and provides space for internal wiring.

B. Development of straight rail module

The developed straight module is illustrated in Fig. 15. The straight module comprising straight and connecting parts at both ends can support large loads and enable a smooth connection. The side plate supports the monitoring robot. A5052 was used as the material, and its structure was pipe-like, making it lightweight and torsionally rigid. The dimensions were obtained by determining the relationship between the dimensions of the cross-section, the weight of the straight module, and the torsional angle of the joint axis. The thickness of the cross-section is 20 mm, the height is 275 mm, and the width is 120 mm. The connecting part has the same arrangement of guide pins and bolts as in the bendable module.

C. Development of basement unit

The basement units (Fig. 16(a)) comprise three rollers: the upper large roller, the side support roller, and the lower large roller. The upper and lower rollers support moment in the pitch direction of the rail, whereas the side rollers support moments in the yaw and roll directions. The lower roller is equipped with a braking mechanism and rubber pads. To ensure portability, each roller had its highly rigid SUS Corp. frame (ZF100 series), each of which is fixed to the ground using an anchor bolt. The upper roller has large legs and is fixed to the floor using 20 M10 bolts.

The pitch angle of the rail can be adjusted by moving the lower large roller up and down using an adjuster. The roll angle of the rail is also adjusted by using an adjuster of the side support roller, but it may not match the change

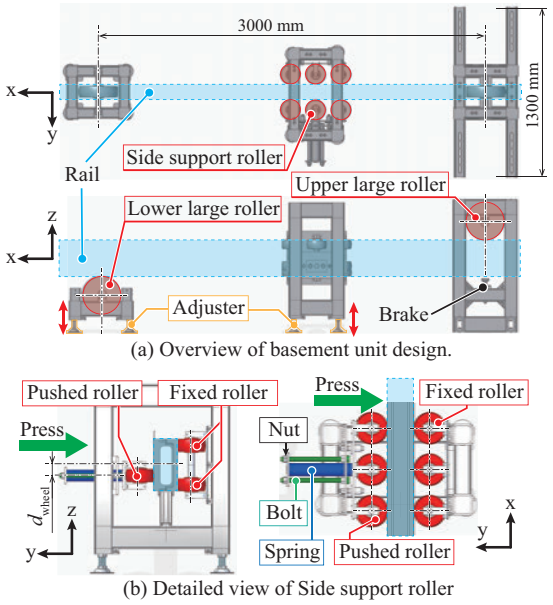

(a) Overview of basement unit design.

(b) Detailed view of Side support roller

Fig. 16. Overview of basement unit design.

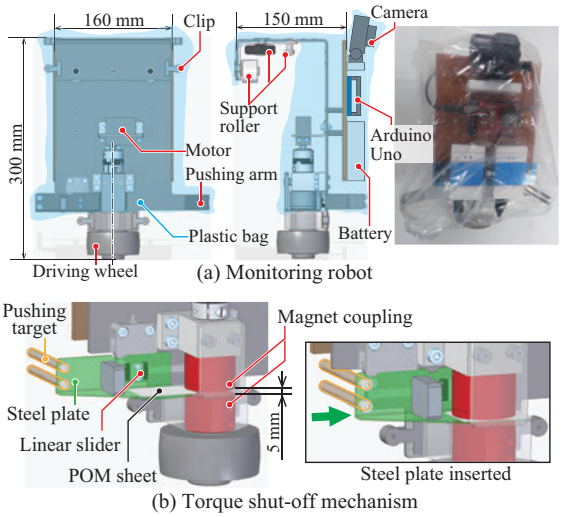

(a) Monitoring robot

(b) Torque shut-off mechanism

Fig. 17. Overview of designed monitoring robot.

in the inclination of the frame owing to changes in the rail width caused by insufficient rigidity of the frame or machining errors. Furthermore, when the rail structure is deployed on a circular arc in the PCV, a large torsional movement in the roll direction occurs because of its weight. The roller pressing mechanism (Fig. 16(b)) presses the rollers against the sides of the rail. It has two pairs of fixed rollers on one side and a spring-loaded roller-pressing mechanism on the other side. To prevent the rail structure from twisting and rotating in the roll direction, bolts and nuts were tightened to press the rollers against the sides of the rail to compensate for the roll misalignment. The rollers are positioned below the center of the rail to generate a large moment.

IV. Development of Monitoring Robot

The monitoring robot is illustrated in Fig. 17. It has a camera (GoPro) and three types of support rollers at the top. The robot is supported by four wheels on the side plate of the rail from both sides and two wheels on the top of the rail to ensure that the robot overhang and support its weight.

The lower part of the robot is equipped with a drive wheel driven by a servomotor (10 W) and controlled by Arduino Uno. The normal operating time is assumed to be 15 hours because the microcontroller fails first due to radiation.

A. Coated with bags for easy disposal

The monitoring robot is covered with a plastic bag to reduce contamination. Drive and support rollers were mounted outside the plastic bag. The drive wheel is attached, and the drive torque is transmitted by placing one side of the magnetic coupling outside the bag, as shown in Fig. 17(a). An air gap of 5 mm is maintained between the magnetic couplings to reduce the load during attachment and removal.

The six support rollers are mounted on a single-sheet metal component, which is attached to the main body of the monitoring robot using a clip over the bag.

B. Design of torque shut-off mechanism

The torque - mechanism is illustrated in Fig. 17(b). The torque transmission of the magnetic coupling is interrupted when the iron plate is inserted between the couplings by the arm of the normal monitoring robot.

To prevent the iron plate from becoming stuck in contact with the magnetic coupling during insertion, the iron plate is attached to the linear slider, and a 0.5 mm thick fluoroplastic sheet is attached to the steel plate to maintain spacing and reduce friction. In addition, a roller plunger is mounted to prevent an unintended start of the steel plate insertion. The plunger fits into a notch in the steel plate and moves only when a certain amount of propulsive force is applied, thereby interrupting torque transmission.

The arm that activates the shut-off mechanism is shown in Fig. 17. It pushes the two bars at the base of the steel plate (yellow poles in Fig. 17(b)).

V. Experiments

A. Assembling experiment of straight module

We verified whether the modules could be connected and pushed out within a standard timeframe using a straight module and basement unit. The procedure for connecting the modules is as follows: (Step.1) Connect cables that pass through the inside of the module. (Step.2) Insert the guide pins into the connecting parts of the module. If it does not fit, use a vise to push the guide pin. (Step.3) Fasting using two M8 bolts. (Step.4) Release the brake from the rail structure and push the rail in the direction of the extension.

Two of the authors (both males in their 20s) wearing helmets and masks performed the connecting and pushing operations on one module, and measured the time required for (Step.1, 2, and 3) of the coupling operation and (Step.4) of the pushing operation, assuming real work. Three trials were conducted and the average value was used to evaluate the results.

The allowable daily exposure of workers was set to 3 mSv. Considering that the radiation dose in the work environment

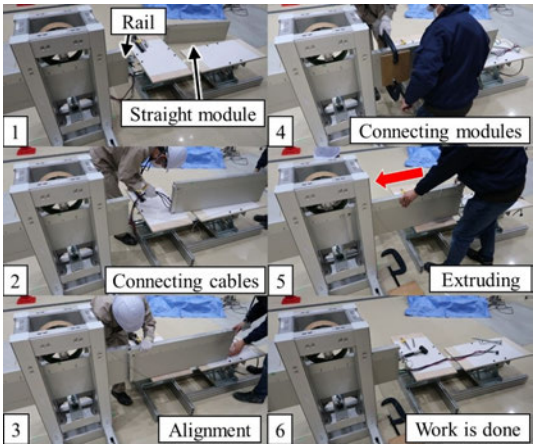

Fig. 18. Snapshots of assembling experiment.

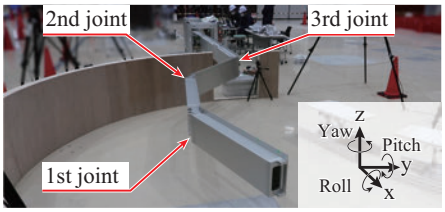

Fig. 19. Snapshot of joint angles control experiment.

was 6 $\mathrm{mSv/h}$, we assumed a safety factor of two, which means that the allowable connection time per module was 15 min. The experimental setup is illustrated in Fig. 18.

The result is as follows: First trial: 6' 46", Second: 5' 58", Third: 4' 36". The average time required for this operation was 5' 47", respectively, which is shorter than the criteria of 15 min. The lightweight straight modules and workbench facilitated the relative positioning of the modules and contributed to quick connection. The large rollers at the base contributed to a smooth extrusion operation.

B. Joint angle control experiment

It was verified whether the angles of the active joints could be controlled to match the command angles. Three bendable and five straight modules were connected to control the joint angles. The roll angle was adjusted with an adjuster in the basement unit while measuring at a level such that the joint between the straight module and bendable rail module was horizontal. Three trials were conducted and the joint angles were measured using the installed potentiometers (Fig. 19).

The time variations in the command and the actual joint angles of each joint are shown in Fig. 20. The result shows that the roll direction posture is adjusted at the basement unit to reduce the moment owing to the dead weight applied to the joints, and the joint angles can follow the command angle with an error of ±1 deg or less. However, tracking the command angle is slow and the control parameters must be improved.

C. Driving experiment of monitoring robot

We verified whether the smooth movement of the monitoring robot on a rail structure could be achieved by attaching

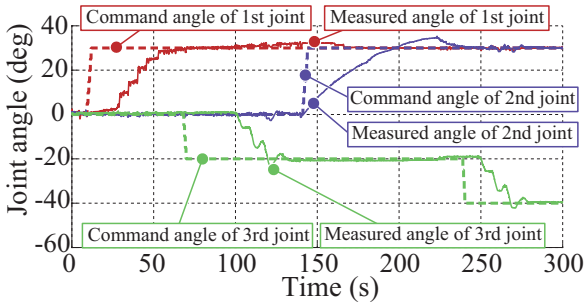

Fig. 20. Sequential data of controlled joint angles.

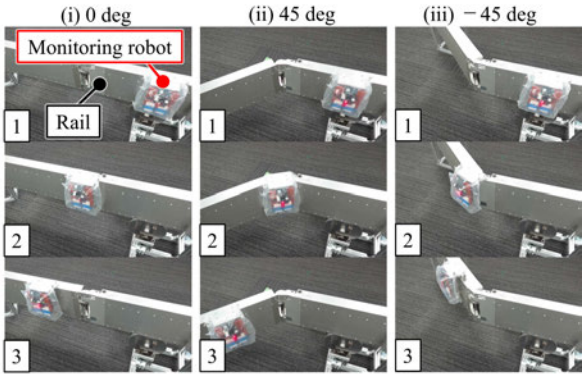

Fig. 21. Snapshots of driving test of the monitoring robot.

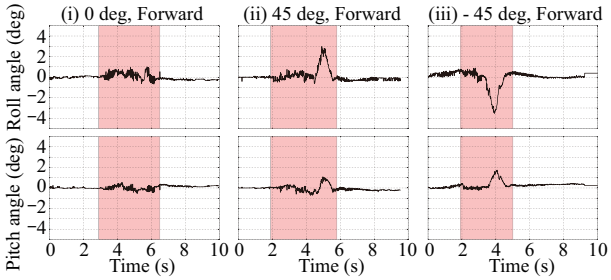

Fig. 22. Sequential data of the monitoring robot posture. Within the red area in the graph, monitoring robots run over the joint parts.

the drive wheels and supporting rollers to the outside of the bag. The criterion is that the variation in the posture angle of the monitoring robot during movement should be within 5 deg. The direction in which the rail structure extends is the x-axis, and the vertically upward direction is the z-axis. The posture angles around the X, Y, and Z axes are the roll, pitch, and yaw angles, respectively. The robot moved forward and backward three times with the joint angles set to 0, 45, and -45 deg. During the experiment, a marker was attached to the monitoring robot, and its position and posture were measured using a motion capture.

The joint passage was achieved in all cases. The forward motion at each angle is shown in Fig. 21. The changes in roll and pitch angles of the monitoring robot are shown in Fig. 22. When the rail structure was bent, the roll and pitch angles of the monitoring robot fluctuated. In all cases, the variation in the attitude angle was within 5 deg, indicating that the rail interpolation mechanism enabled the smooth monitoring.

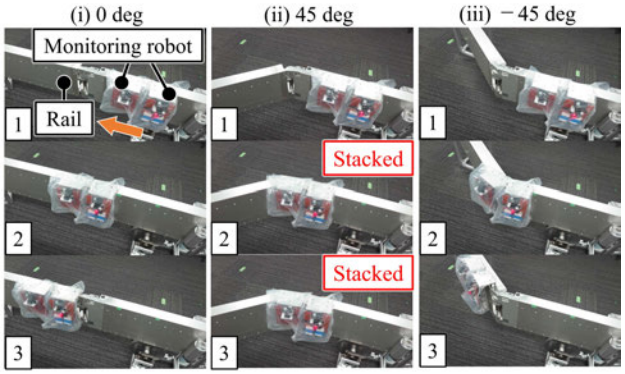

Fig. 23. Snapshots of propelling experiment.

D. Disposing experiment of monitoring robot

We verified whether the torque shut-off mechanism of the monitoring robot enable the propelling of the failed robot as shown in Fig. 23. The monitoring robot was propelled by another robot. Three trials were conducted with joint angles set to 0, 45, and -45 deg. Two types of steel plates with thicknesses of 0.8 and 1.6 mm were used. The success rates are as follows: zero out of three with 0.8 mm steel plate in three joint angles, three out of three with 1.6 mm in only 0 and -45 deg situations.

The 0.8 mm steel plate was successfully inserted, but the magnetic force was not sufficiently blocked; the robot became stuck before reaching the joint in all three situations. The experiment with a steel plate thickness of 1.6 mm is shown in Fig. 23. The robot is propelled on all three trials when the joint angles are 0 and -45 deg. The results show that the back drivability is improved by inserting a steel plate of sufficient thickness between the magnetic couplings, and the propulsion of the failed robot can be partially realized.

However, the monitoring robot failed to be propelled in all cases at 45 deg. This was because the support roller of the failed monitoring robot was stuck in the bending area of the rail structure, which caused a force in the direction of lifting the robot even when the normal robot is pushed from behind. Because a failed robot must be propelled by a normal robot when multiple robots fail, it is necessary to consider a drive wheel that does not get stuck easily and an arm shape that allows force to be applied correctly in the direction of travel.

VI. Conclusion

We verified the feasibility of "Rail DRAGON," a bendable, ultra-long modular rail system with high workability and portability, for easy installation and disposal of observation equipment. We developed a highly rigid straight module and basement unit that can compensate for the inclination of the entire rail. Experimental results showed that the error of the joint angle from the command angle was less than ±1 deg and that active joint control by a lightweight actuator could be realized by adjusting the entire rail posture horizontally. We developed a connecting part of a rail module that can be connected by pin insertion and bolt fastening and a basement unit that supports the rail using rollers. Experiments have shown that the connection and extrusion of one module can be completed within 6 min.

A monitoring robot that hangovers the side plates of a rail was developed. The joints are equipped with a mechanism that interpolates the side plates according to the joint angle. The experimental results showed that the robot's posture angle fluctuation during movement could be suppressed to less than 5 deg, enabling smooth movement of the monitoring robot without being restrained by the rail structure. A torque shut-off mechanism using a magnetic coupling and a steel plate was developed. In the experiment, it was found that both covering the bag and variable back drivability could be achieved.

Future tasks include propelling multiple failed monitoring robots and verifying the feasibility of dismantling monitoring robots using a teleoperated robot.

References

[1] Y. Yokokohji, "The use of robots to respond to nuclear accidents: Applying the lessons of the past to the fukushima daiichi nuclear power station," *Annual Review of Control, Robotics, and Autonomous Systems*, vol. 4, pp. 681–710, 2021.

[2] R. Hanabusa and et al, "3D map generation for decommissioning work," in *Proc. IEEE International Conference on Intelligent Autonomous Systems*, 2020, pp. 46–50.

[3] IRID, "R&D topics development of robot "PMORPH"for investigation in- side unit 1 primary containment vessel (PCV)," 2017. [Online]. Available: http://irid.or.jp/en/topics/

[4] Y. Bai and et al, "Research of environmental modeling method of coal mine rescue snake robot based on information fusion," in *Proc. IEEE International Conference on Information Fusion*, 2017, pp. 1–8.

[5] G. Endo and et al, "Super dragon: A 10-m-long-coupled tendon-driven articulated manipulator," *IEEE Robotics and Automation Letters*, vol. 4, no. 2, pp. 934–941, 2019.

[6] Y. Ueno and et al, "Development of hiryu-ii: A long-reach articulated modular manipulator driven by thrusters," *IEEE Robotics and Automation Letters*, vol. 5, no. 3, pp. 4963–4969, 2020.

[7] B. Haist and et al, "Remote handling preparations for jet ep2 shutdown," *Fusion Engineering and Design*, vol. 84, no. 2-6, pp. 875–879, 2009.

[8] R. Fukui and et al, "Automated construction system of robot locomotion and operation platform for hazardous environments—basic system design and feasibility study of module transferring and connecting motions," *Journal of Field Robotics*, vol. 33, no. 6, pp. 751–764, 2016.

[9] S. Okada and et al, "Development of advanced measurement technologies and their application to decommissioning of fukushima daiichi nuclear power station," 2022, accessed on 25 Jul. 2023. [Online]. Available: https://www.hitachi.com/rev/archive/2022/r2022_04/04c03/index.html

[10] J.-P. Merlet and et al, "A portable, modular parallel wire crane for rescue operations," in *Proc. IEEE International Conference on Robotics and Automation*, 2010, pp. 2834–2839.

[11] A. Nakayoshi and et al, "Review of fukushima daiichi nuclear power station debris endstate location in oecd/nea preparatory study on analysis of fuel debris (preades) project," *Nuclear Engineering and Design*, vol. 369, p. 110857, 2020.

[12] Z. Jiang and et al, "An improved robot calibration method using the modified adjoint error model based on poe," *Advanced Robotics*, vol. 34, no. 19, pp. 1229–1238, 2020.

[13] IAEA, "Classification of radioactive waste," 2009, accessed on 25 Jul. 2023. [Online]. Available: https://www.iaea.org/publications/8154/classification-of-radioactive-waste

[14] Y. Fujimoto and et al, "On a high-backdrivable direct-drive actuator for musculoskeletal bipedal robots," in *Proc. IEEE International Workshop on Advanced Motion Control*, 2010, pp. 389–395.

[15] H. Kaminaga and et al, "Backdrivability analysis of electro-hydrostatic actuator and series dissipative actuation model," in *Proc. IEEE international conference on robotics and automation*, 2010, pp. 4204–4211.

[16] O.-P. Kahkonen and et al, "Radiation damage in Nd-Fe-B magnets: temperature and shape effects," *Journal of Physics: Condensed Matter*, vol. 4, no. 4, p. 1007, 1992.